

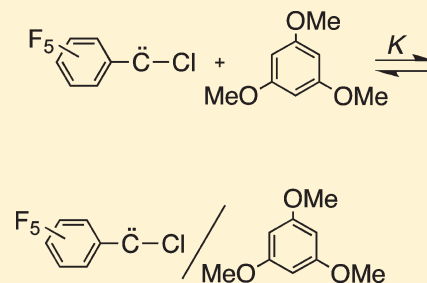
Trimethoxybenzene Complexes of Pentafluorophenylchlorocarbene

Lei Wang, Robert A. Moss,* and Karsten Krogh-Jespersen*

Department of Chemistry and Chemical Biology, Rutgers, The State University of New Jersey, New Brunswick, New Jersey 08903, United States

Supporting Information

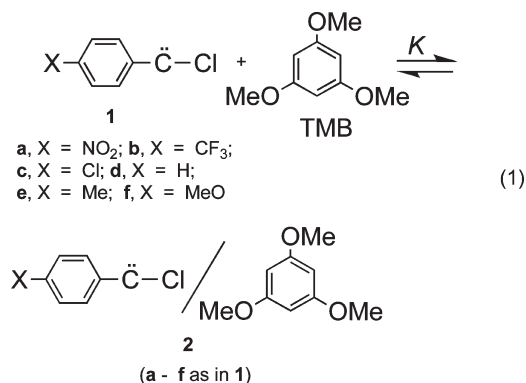
ABSTRACT: Pentafluorophenylchlorocarbene, generated by laser flash photolysis (LFP) of pentafluorophenylchlorodiazirine, formed π -type complexes with 1,3,5-trimethoxybenzene in pentane. The carbene and carbene complexes were in equilibrium with $K = 3.21 \times 10^5 \text{ M}^{-1}$ at 294 K. From the temperature dependence of K , $\Delta H^\circ = -10.2 \text{ kcal/mol}$, $\Delta S^\circ = -9.5 \text{ eu}$, and $\Delta G^\circ = -7.4 \text{ kcal/mol}$ at 298 K. The carbene complexes were characterized by UV-vis spectroscopy and computational analysis.



I. INTRODUCTION

Given the formally vacant p-orbital featured by singlet carbenes, we expect that electron donation by solvents will lead to at least transient carbene-solvent complexes. Indeed, indirect evidence for such complexation has been offered in the context of the solvent modulation of carbenic reactivity.¹ More recently, direct evidence for carbene complexation has accrued using such physical methods as calorimetry,² IR spectroscopy,³ and UV spectroscopy,⁴ coupled with fast laser technology.

We provided the first direct spectroscopic evidence for carbene-carbene complex equilibration; see eq 1.⁵ Phenylchlorocarbene (PhCCl, **1d**) formed a π -type complex with 1,3,5-trimethoxybenzene (TMB),

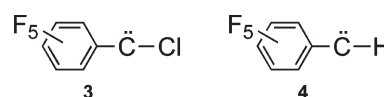


and the carbene and carbene complex were in equilibrium with $K = 1264 \text{ M}^{-1}$. From the temperature dependence of K , we extracted the associated thermodynamic parameters: $\Delta H^\circ = -7.1 \text{ kcal/mol}$, $\Delta S^\circ = -10.2 \text{ eu}$, and $\Delta G^\circ = -4.1 \text{ kcal/mol}$.⁵

Very recently, we extended this study to the *p*-substituted phenylchlorocarbenes **1a–f**, where $X = \text{NO}_2$, CF_3 , Cl , H , Me , and MeO .⁶ Logarithms of the equilibrium constants were

well-correlated by the Hammett σ_p constants for X , with $\rho = 2.48$.⁶ The positive value of ρ suggests that electron-withdrawing groups destabilize carbenes **1a–1f**, shifting the equilibrium toward complexes **2a–2f**, where TMB donates electron density to the vacant carbenic p-orbital. Also, stronger charge-transfer complexes **2a–2f** will form when the electron-rich TMB interacts with the more electron-deficient carbene centers and aromatic rings induced by an electron-withdrawing substituent.⁶

The pentafluorophenyl group (C_6F_5) is more electron-withdrawing than the phenyl group (C_6H_5): σ_I of C_6F_5 is 0.31 compared to 0.12 for C_6H_5 ,⁷ and σ_{R^+} of C_6F_5 is -0.07 ⁸ compared to -0.17 ⁹ or -0.30 ¹⁰ for C_6H_5 . On the basis of our previous analysis,⁶ pentafluorophenylchlorocarbene ($\text{F}_5\text{-PhCCl}$, **3**) should bind more strongly than PhCCl to TMB. Indeed, our electronic structure calculations (see below) indicate that $\text{F}_5\text{-PhCCl/TMB}$ complexes should be approximately 3–5 kcal/mol more stable in enthalpy and free energy than PhCCl/TMB complexes.



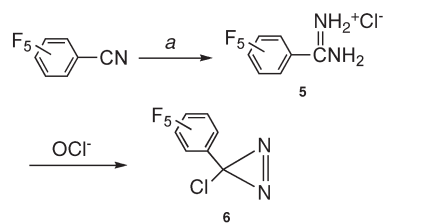
Although pentafluorophenylcarbene ($\text{C}_6\text{F}_5\text{CH}$, **4**) is known,¹¹ $\text{F}_5\text{-PhCCl}$ is not. Carbene **4** is a ground state triplet with (an experimental) $\Delta G_{S-T} = -3.1 \text{ kcal/mol}$ at 298 K,¹¹ but preferential stabilization of singlet **3** by electron donation from its chlorine substituent should make the singlet the ground state. Indeed, our CCSD(T) calculations predict $\Delta G_{S-T} = 4.2 \text{ kcal/mol}$ for **3** but -5.6 kcal/mol for **4** (see below). An analogous reversal of ground state multiplicity is found with phenylcarbene (PhCH) and PhCCl, where prior computational studies

Received: April 28, 2011

Revised: May 27, 2011

Published: June 22, 2011

Scheme 1. Preparation of Pentafluorophenylchlorodiazirine



(a) MeAl(Cl)NH₂ in toluene (80 °C); then SiO₂, H₂O.

support a triplet ground state for PhCH ($\Delta G_{S-T} \sim -4$ kcal/mol)¹² but a singlet ground state for PhCCl ($\Delta G_{S-T} = 7.8$ kcal/mol).¹³ Our computed CCSD(T) ΔG_{S-T} values for PhCH and PhCCl are -4.5 and 7.7 kcal/mol, respectively, and thus agree fully with the results of the prior studies.

To test our computational prediction that F₅-PhCCl will bind more tightly to TMB than PhCCl, we require a synthesis of pentafluorophenylchlorodiazirine, which would serve as a photochemical precursor for F₅-PhCCl. The desired precursor was prepared by the sequence of Scheme 1: commercially available pentafluorobenzonitrile was converted by Garigipati's reaction¹⁴ to pentafluorobenzamidine (**5**), and the latter was converted to pentafluorophenylchlorodiazirine (**6**) by Graham oxidation with aqueous hypochlorite.¹⁵ Experimental details for these procedures appear in the Experimental section.

2. EXPERIMENTAL DETAILS AND COMPUTATIONAL METHODS

2.1. Experimental Details. *Preparation of Pentafluorobenzamidine (5).*¹⁴ A solution of 2 M trimethylaluminum in toluene (100 mL) was slowly added to a magnetically stirred suspension of 11.7 g (0.22 mol) of ammonium chloride in 40 mL of dry toluene under nitrogen at 0 °C. After addition, the mixture was warmed to room temperature and stirred for 1 h until gas evolution ceased. Then, 29 g (0.15 mol) of pentafluorobenzonitrile in 50 mL of dry toluene was slowly added, and the solution was heated to 80 °C for 48 h under nitrogen. The reaction was then quenched by slow addition of 100 mL of methanol at 0 °C. The reaction mixture was slowly poured into a slurry of 30 g of silica gel in 80 mL of chloroform and stirred for 1 h. The silica gel was filtered and washed with methanol. The combined filtrate and wash were stripped of solvent on the rotary evaporator leaving a residue, which was a mixture of pentafluorobenzamidine chloride and ammonium chloride. The residue was extracted twice with 400 mL portions of 1:10 methanol–chloroform. The combined extracts were stripped to yield 10 g (27%) of pentafluorobenzamidine chloride **5**, mp 272–276 °C (dec.).

IR (film, cm⁻¹): 2978, 2932, 1452, 1448, 1433, 1321, 1317, 1004, 984, 943.

¹⁹F NMR (470 MHz, DMSO-*d*₆, δ): -138.45 and -138.50 (d, 2F); -147.88 , -147.93 , and -147.99 (t, 1F); -160.23 , -160.26 , -160.28 , and -160.31 (m, 2F).

¹³C NMR (125 MHz, DMSO-*d*₆, δ): 155.50 (s, C=N); 145.32 and 143.32 (d of m); 144.07 and 142.37 (d of m); 138.71 and 136.70 (d of m); 106.39 (t).

*Preparation of 3-Chloro-3-pentafluorophenyldiazirine (6).*¹⁵ A mixture of 5 g of LiCl, 2.0 g (8.1 mmol) of amidine **5**, and 50 mL of DMSO was stirred until most of the LiCl had dissolved. Then, 100 mL of pentane was added, followed by slow addition at room

Table 1. Singlet–Triplet Separation (ΔG_{S-T} , kcal/mol)^a in CH₂, PhCH, F₅-PhCH, PhCCl, and F₅-PhCCl^b

species	B97D	wB97XD	M06-2X	B3LYP	CCSD(T) ^c
CH ₂	-12.0	-12.3	-14.2	-11.8	-12.9
PhCH	-6.6	-7.1	-8.0	-5.8	-4.5
F ₅ -PhCH	-6.7	-8.2	-9.1	-7.0	-5.6
PhCCl	4.3	3.8	4.8	5.2	7.7
F ₅ -PhCCl	0.35	-0.40	0.80	0.70	4.2

^a A negative value for this quantity signifies that the triplet state is more stable than the singlet state. ^b 6-311+G(d) basis sets used in all calculations, see Computational Methods. ^c The electronic to free energy corrections obtained at the B3LYP level were applied to the electronic energies obtained from CCSD(T) calculations to arrive at approximate CCSD(T) free energies.

temperature of 100 mL of 12% aqueous NaOCl (commercial bleach), saturated with NaCl. Stirring was continued for 2 h at room temperature. The pentane phase was separated and retained, and the aqueous phase was extracted twice with 50 mL portions of pentane. The combined pentane solutions were dried over MgSO₄, concentrated to ~ 5 mL, and chromatographed over a short column of silica gel using pentane as the eluent. We thus obtained 1.1 g of diazirine **6** (in pentane solution), 56% yield.

UV (pentane): 326, 333, 342 nm; see Figure S-1 in the Supporting Information.

IR (film, cm⁻¹): 1584 (N=N).¹⁵

¹³C NMR (125 MHz, CDCl₃, δ): 36.604 (s), 110.18 (m), 139.13 and 137.10 (dm, ¹J_{C-F} = 254 Hz), 144.60 and 142.54 (dm, ¹J_{C-F} = 258 Hz), 147.11 and 145.07 (dm, ¹J_{C-F} = 256 Hz).

¹⁹F NMR (470 MHz, DMSO-*d*₆, δ): -139.36 and -139.40 (d of m, 2F); -149.06 , -149.11 , and -149.16 (t of m, 1F); -159.81 , -159.85 , and -159.90 (t of m, 2F).

2.2. Computational Methods. Electronic structure calculations were carried out using methodologies implemented in the Gaussian 09 suite of programs.¹⁶ Density functional theory (DFT) provided the default methods for the calculation of ground and excited state structures and energetics.¹⁷ Ground state geometry optimizations of carbene and solvent monomers and dimeric carbene–solvent complexes were carried out using the dispersion-corrected B97D,¹⁸ M06-2X,¹⁹ or wB97XD²⁰ exchange–correlation functionals and 6-311+G(d)²¹ basis sets (B97D/6-311+G(d), etc.). The potential energy surfaces for the carbene–solvent complexes are very soft with respect to relative motion of the aryl rings, and the structural minima possess several low-frequency vibrational modes. Hence, all geometry optimizations and normal mode calculations were conducted with tight convergence criteria (opt=tight) imposed and integration grid sizes increased beyond their default values (integral(grid=ultrafine)). Stationary points were characterized by normal-mode analysis, and the (unscaled) vibrational frequencies formed the basis for the calculation of vibrational zero-point energy (ZPE) corrections. Standard thermodynamic corrections (based on harmonic oscillator/rigid rotor approximations and ideal gas behavior) were then applied to convert from purely electronic energies (*E*) to (standard) enthalpies (*H*^o; *T* = 298.15 K) and free energies (*G*^o; *T* = 298.15 K, *P* = 1 atm).²²

Interaction energies of carbene–solvent complexes were approximately corrected for basis set superposition errors (BSSE) through the application of the counterpoise correction.²³ Carbene singlet–triplet energy separations were

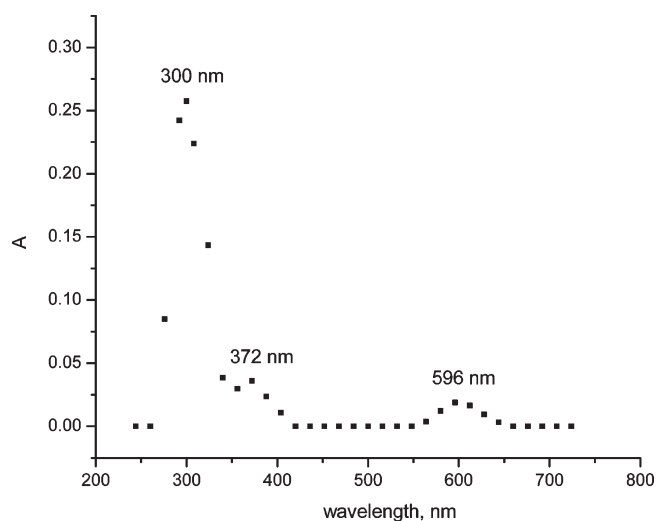


Figure 1. Calibrated UV–vis spectrum of F_5 -PhCCl (**3**) in pentane 150 ns after the laser flash; π (phenyl) \rightarrow p(carbene) absorptions at 300 and 372 nm, σ (carbene) \rightarrow p(carbene) absorption at 596 nm.

evaluated at the B3LYP²⁴ and CCSD(T)²⁵ levels of theory with 6-311+G(d) basis sets (Table 1). Electron population analysis made use of the conventional Mulliken partitioning scheme.²⁶

Excited state calculations (transition wavelengths (λ) and oscillator strengths (f) at optimized B97D ground state geometries utilized the time-dependent DFT formalism^{27a} and the B3LYP functionals (TD-B3LYP/6-311+G(d)//B97D/6-311+G(d)). General solvent effects were incorporated with the polarizable conductor self-consistent reaction field model (CPCM)²⁸ and default parameters for *n*-pentane provided in Gaussian 09. The assignment of a particular electronic transition ($\sigma \rightarrow p$, $\pi \rightarrow p$, or $\pi \rightarrow \pi^*$) was based on inspection of the largest transition amplitudes for the excitation and by visualization of the contributing molecular orbitals (MOs).

3. RESULTS AND DISCUSSION

3.1. Pentafluorophenylchlorocarbene and Complex Formation with Trimethoxybenzene. The laser flash photolysis (LFP) of diazine **6** in pentane gave F_5 -PhCCl (**3**), whose calibrated²⁹ UV–vis spectrum (Figure 1) displayed strong and weak π (phenyl) \rightarrow p(carbene) absorptions at 300 and 372 nm, together with a weak $\sigma \rightarrow p$ absorption at 596 nm. Our electronic structure calculations show that the 300 and 372 nm bands represent charge-transfer type transitions from the nearly degenerate set of high-lying phenyl π -orbitals (e_{1g} symmetry in benzene) to the vacant carbeneic p-orbital (lowest unoccupied molecular orbital (LUMO) in **3**). The MO with a nonzero coefficient on C_1 (phenyl) provides the intense 300 nm band, whereas the other MO gives rise to the much weaker band at 372 nm. The absorptions are computed³⁰ at 296 nm ($f = 0.33$) and 362 nm ($f = 0.042$), respectively. The long wavelength band at 596 nm (computed too far to the red at 867 nm, $f = 0.003$) is principally associated with electron promotion from the carbeneic carbon's filled σ -orbital (highest occupied molecular orbital (HOMO) in **3**) to its vacant p-orbital. The interaction between the aryl π -orbitals and the carbene p-orbital leads to B3LYP computed σ -p (HOMO–LUMO) separations which are too small, as noted by us previously.⁴ The general tendency of DFT to underestimate the HOMO–LUMO separation for weakly

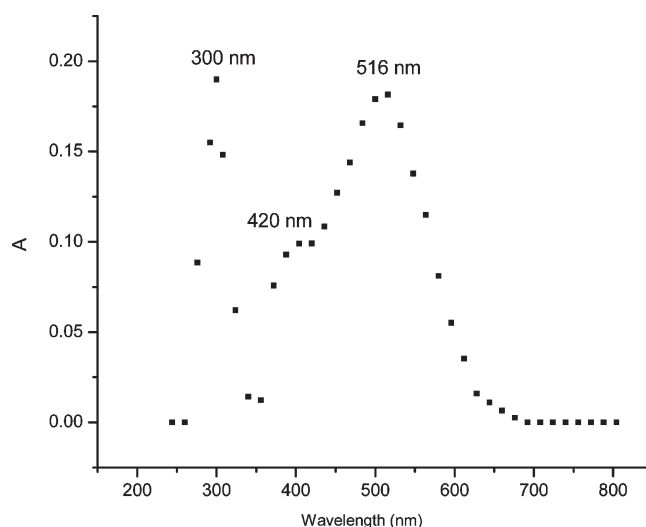


Figure 2. Calibrated UV–vis spectrum acquired 150 ns after LFP generation of F_5 -PhCCl in 0.0128 mM TMB/pentane solution; F_5 -PhCCl absorption at 300 nm; absorption by F_5 -PhCCl/TMB complexes A and B (see Figure 3) at 420 and 516 nm.

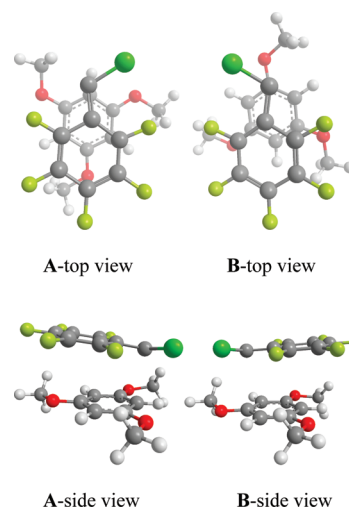


Figure 3. Top and side views of computed π -complexes of high stability formed between F_5 -PhCCl and TMB (in perspective, carbene on top; light green, fluorine; dark green, chlorine; red, oxygen).

interacting systems and thus of TD-DFT to underestimate the electronic excitation energies, when local, time-independent functionals are employed, has been documented.^{27b}

For PhCCl, analogous transitions are observed at 308 and 578 nm⁵ and computed at 292 nm ($f = 0.44$) and 737 nm ($f = 0.002$). The weak $\pi \rightarrow p$ PhCCl transition is computed at 330 nm ($f = 0.032$) but not observed because it is buried beneath the much stronger $\pi \rightarrow p$ band at 308 nm. In F_5 -PhCCl, the weak $\pi \rightarrow p$ absorption is shifted 30–40 nm to the red and is observed as a separate peak at 372 nm (Figure 1).

The LFP of diazine **6** in the presence of 0.0128 mM TMB affords the calibrated UV–vis spectrum shown in Figure 2, with distinct absorptions at 300, 420, and 516 nm. Computational analysis (see below) assigns the 420 and 516 nm absorptions to F_5 -PhCCl/TMB π -complexes A and B, respectively; see Figure 3. Computed absorptions³⁰ for A and B are at 443 nm ($f = 0.16$) and

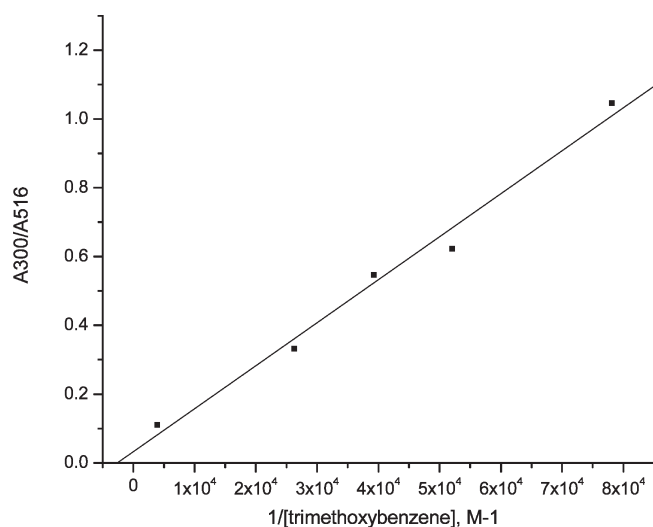
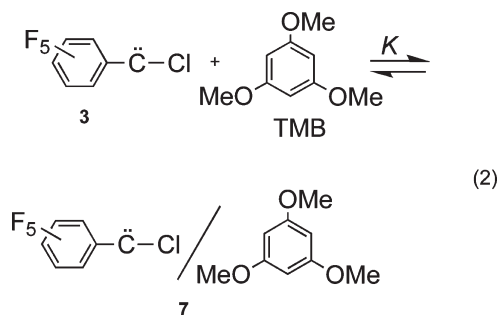


Figure 4. Relative absorption intensities at 300 nm/516 nm vs $1/[\text{TMB}]$ (M^{-1}) for the LFP generation of $\text{F}_5\text{-PhCCl}$ in TMB/pentane solution at 294 K. The slope of the correlation line is $1.25 \times 10^{-5} \text{ M}$ ($r = 0.993$), leading to $K = 3.21 \times 10^5 \text{ M}^{-1}$ for eq 2.³¹

545 nm ($f = 0.083$), respectively. The apparent intensity reversal between the observed and computed A and B absorptions is precedented.⁶

The relative intensities of the $\text{F}_5\text{-PhCCl}$ absorption at 300 nm and the $\text{F}_5\text{-PhCCl}$ /TMB complex absorptions at 420 and 516 nm vary with TMB concentration in a manner consistent with the carbene (3)–carbene complex (7) equilibrium expressed in eq 2; see Figures S-3 to S-6 in the Supporting Information.



Indeed, a plot of the quotient of the calibrated absorption intensities for $\text{F}_5\text{-PhCCl}$ at 300 nm and carbene complex B at 516 nm versus $1/[\text{TMB}]$ at 294 K affords the linear correlation of Figure 4, where the slope ($1.25 \times 10^{-5} \text{ M}$) leads to a value $K = 3.21 \times 10^5 \text{ M}^{-1}$ for the equilibrium constant of eq 2.³¹

Given that the reaction of $\text{F}_5\text{-PhCCl}$ with TMB produces complex A in addition to complex B, the actual equilibrium constant for eq 2 will be somewhat larger than $3.21 \times 10^5 \text{ M}^{-1}$, which is based solely on the formation of complex B. The formation of the $\text{F}_5\text{-PhCCl}$ /TMB complexes from carbene 3 and TMB is not only thermodynamically favorable ($K \gg 1$) but is also ~ 250 times more favorable than formation of the corresponding PhCCl /TMB complexes for which $K = 1.26 \times 10^3 \text{ M}^{-1}$ ($\Delta\Delta G^\circ \sim 3.3 \text{ kcal/mol}$).^{5,32}

3.2. Enthalpy and Entropy of Complexation. We determined K for eq 2 at four additional temperatures (see Figures S-7 to S-10 in the Supporting Information), obtaining the following values of K (M^{-1}): 2.39×10^6 at 263 K; 6.52×10^5 at 281 K;

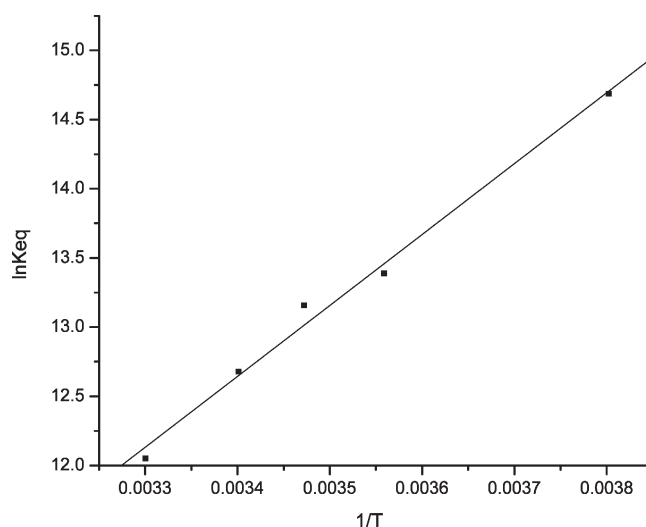


Figure 5. Plot of $\ln K$ (M^{-1}) vs $1/T$ (K^{-1}) for the equilibrium of eq 2. The slope (5126) affords $\Delta H^\circ = -10.2 \text{ kcal/mol}$, and the intercept (-4.78) gives $\Delta S^\circ = -9.5 \text{ eu}$. The correlation coefficient is $r = 0.996$.

5.17×10^5 at 288 K; and 1.71×10^5 at 303 K. A correlation of $\ln K$ vs $1/T$ appears in Figure 5, from which the slope and intercept give $\Delta H^\circ = -10.2 \pm 0.6 \text{ kcal/mol}$ and $\Delta S^\circ = -9.5 \pm 1.9 \text{ eu}$, respectively, leading to $\Delta G^\circ = -7.4 \pm 0.8 \text{ kcal/mol}$ at 298 K.

From these results, the complexation of $\text{F}_5\text{-PhCCl}$ by TMB is about 3 kcal/mol more favorable in both enthalpy and free energy than complexation of PhCCl . Our computational prediction (see above and below) is for energetic advantages favoring the complexation of $\text{F}_5\text{-PhCCl}$ by $\sim 4 \text{ kcal/mol}$ in ΔG° and 3.7–5.3 kcal/mol in ΔH° , so that the experimental and computational results are in quite good agreement.

3.3. Computational Studies. We first determined the ground state spin multiplicity of $\text{F}_5\text{-PhCCl}$ and related carbenes by evaluating the energies of the singlet (S, σ^2 occupancy) and triplet (T, $\sigma^1 p^1$ occupancy) states at their respective optimized geometries. DFT results for the S-T free energy separations of CH_2 , PhCH , $\text{F}_5\text{-PhCH}$ (4), PhCCl (1d), and $\text{F}_5\text{-PhCCl}$ (3) obtained with the 6-311+G(d) basis set and B97D, M06-2X, wB97XD, or B3LYP functionals are shown in Table 1. We also present wave function based CCSD(T)/6-311+G(d) results obtained from single point calculations using the B3LYP/6-311+G(d) optimized geometries of these carbenes. S-T potential energy differences are available in Table S-1 in the Supporting Information.

All five computational methods applied here clearly predict that PhCH and $\text{F}_5\text{-PhCH}$ possess triplet ground states. Perfluorination of the aryl ring increases the S-T separation uniformly by ca. 1 kcal/mol, except in the B97D calculations that show virtually no change ($\sim 0.1 \text{ kcal/mol}$). For PhCCl , the computational methods again agree and uniformly predict a singlet ground state for this carbene. The preferential stabilization of the triplet state by perfluorination of the aryl ring is larger for $\text{F}_5\text{-PhCCl}$ ($\sim 3.5\text{--}4.5 \text{ kcal/mol}$) than $\text{F}_5\text{-PhCH}$ ($\sim 0.1\text{--}1.2 \text{ kcal/mol}$). The DFT methods predict a S-T separation less than 1 kcal/mol for $\text{F}_5\text{-PhCCl}$; the application of the wB97XD functionals actually predicts, albeit barely, a triplet ground state for $\text{F}_5\text{-PhCCl}$. In contrast, our CCSD(T) calculations arrive conclusively at a singlet ground state for $\text{F}_5\text{-PhCCl}$ with $\Delta G_{\text{S-T}} = 4.2 \text{ kcal/mol}$.

Table 2. Computed Thermodynamic Parameters for F₅-PhCCl/TMB Complexes A and B

species/method	$\Delta H^{\circ a}$	$\Delta S^{\circ a}$	$\Delta G^{\circ a,b}$	$\Delta H(\text{corr})^{\circ a,c}$
A/B97D	-17.6	-40.8	-5.4	-13.5
A/M06-2X	-16.2	-37.6	-5.0	-11.9
A/wB97XD	-14.9	-37.5	-4.3	-11.1
B/B97D	-14.8	-37.4	-3.6	-11.2
B/M06-2X	-15.3	-37.3	-4.2	-11.3
B/wB97XD	-13.7	-36.1	-1.6	-10.2

^a ΔH° and ΔG° in kcal/mol, ΔS° in eu, relative to the separated reactants; $T = 298.15$ K. ^b The free energy differences were computed using a reference state of 1 M concentration for each species participating in the reaction. ^c Counterpoise-corrected enthalpies.

It is well-accepted that single-determinant methods (HF or DFT) tend to overestimate the stability of high spin states and that extensive recovery of electron correlation energy through, for example, configuration interaction must be made to correct this bias.³³ The CCSD(T) derived values for the singlet–triplet (S-T) separations in PhCH (-4.5 kcal/mol) and F₅-PhCH (-5.6 kcal/mol) match the experimentally derived values fairly well (-2 to -3 kcal/mol for PhCH, ~ -4 kcal/mol for F₅-PhCH),^{11,34,35} although they still lean toward an exaggerated preference for the triplet state. A comparison of our computed DFT and CCSD(T) results for ΔG_{S-T} in the aryl carbenes (Table 1) shows a further systematic overestimation of relative triplet state stability by DFT of ca. 2–4 kcal/mol. The experimental S-T separation in methylene (CH₂) is -9.1 kcal/mol (triplet ground state);³⁶ the computational methods used here, including CCSD(T), predict a methylene S-T separation larger by 3–5 kcal/mol (Table 1). Thus, the S-T separation in F₅-PhCCl (3) should be even larger than the CCSD(T) predicted value of 4.6 kcal/mol and could approach 7–9 kcal/mol.

We have previously documented that arylhalocarbenes and TMB preferentially form sandwich-type π -complexes (viz., prototype complexes A and B in Figure 3) and that more spatially extended complexes of the *O*-ylidic type are slightly higher in energy (2–3 kcal/mol above A or B) and not competitive. In the A π -complex, the carbene center interacts strongly with an unsubstituted carbon of TMB (C2); for example, the computed C(carbene)–C2(TMB) distance is 2.72 Å (B97D/6-311+G(d)), while the C(carbene)–C1(TMB) separation is 3.09 Å. In the B complex, the carbene center interacts with the C1–C2 bond of TMB; the C(carbene)–C1 and C2 (TMB) distances are 3.07 and 3.04 Å, respectively. Substantial stabilizing face-to-face overlap originates between the aromatic ring moieties, in particular for complexes of type A. The net charge transferred from TMB to F₅-PhCCl is 0.21 e in A and 0.12 e in B.

Density functionals, which explicitly include dispersion corrections, provide appropriate binding energies of arylhalocarbene/TMB complexes.^{5,6} The computed energetic parameters for the F₅-PhCCl/TMB complexes A and B are shown in Table 2. The binding enthalpies and free energies are systematically slightly more favorable for type A than type B complexes by 1–2 kcal/mol. According to our interpretation of the spectroscopic data, the measured equilibrium constant is associated with B type complexes for which our B97D, M06-2X, and wB97XD calculations predict binding enthalpies $\Delta H^{\circ} = -11.2$, -11.3 , and -10.2 kcal/mol, respectively (Table 2). These computed enthalpies compare very favorably with the measured value ($\Delta H^{\circ} = -10.2 \pm 0.6$ kcal/mol), and they are

Table 3. Electronic Transition Wavelengths (λ , nm) and Oscillator Strengths (f , Dimensionless) Computed at the TD-B3LYP/6-311+G(d)//B97D/6-311+G(d) Level with CPCM Solvent Corrections (*n*-Pentane)

λ, f	F ₅ -PhCCl	complex A	complex B
λ_1, f_1	867, 0.003	775, 0.018	823, 0.016
λ_2, f_2	362, 0.042	550, 0.003	609, 0.004
λ_3, f_3	296, 0.332	443, 0.161	545, 0.083
λ_4, f_4	292, 0.048	338, 0.068	357, 0.032
λ_5, f_5	279, 0.020	330, 0.061	346, 0.039

slightly more than 3 kcal/mol larger than the analogously calculated binding enthalpies of PhCCl/TMB type B complexes (-7.5, -8.0, and -7.0 kcal/mol, respectively). The computed entropies are numerically much larger than the experimentally determined ones, most likely due to the difference in physical phase serving as reference for the calculations (gas) and experiments (condensed). It seems likely that some molecular degrees of freedom have effectively been frozen out in the solution phase, before carbene–solvent complex formation occurs. Generally, the computed ΔG° values are more favorable for type B F₅-PhCCl/TMB than PhCCl/TMB complexes by approximately 4 kcal/mol, corresponding to an increase in equilibrium constant by a factor of $\sim 10^3$; the experimental estimate is ~ 250 (see above).

Computed UV–vis transitions for F₅-PhCCl and complexes A and B are presented in Table 3. The lowest energy transition (λ_1) retains the $\sigma \rightarrow p$ label in all three species, although the “carbenic” σ and p -orbitals attain some Cl and phenyl π -character, respectively, from orbital mixing. The intense 296 nm F₅-PhCCl transition as well as the F₅-PhCCl/TMB complex signature transitions at 443 nm (complex A) and 545 nm (complex B) may all be assigned as $\pi \rightarrow p$ transitions; hence they carry considerable charge transfer character. Finally, we note that it is the intensities of these latter transitions (f_3 , Table 3) that are employed when determining the value of the experimental equilibrium constant (see the Supporting Information).

4. CONCLUSIONS

Pentafluorophenylchlorocarbene, generated by laser flash photolysis of pentafluorophenylchlorodiazirine, formed π -type complexes with 1,3,5-trimethoxybenzene in pentane. The carbene and carbene complexes were in equilibrium with $K = 3.21 \times 10^5$ M⁻¹ at 294 K. The thermodynamic parameters for the equilibrium were determined from the temperature dependence of K : $\Delta H^{\circ} = -10.2$ kcal/mol, $\Delta S^{\circ} = -9.5$ eu, and $\Delta G^{\circ} = -7.4$ kcal/mol at 298 K. The carbene complexes were characterized by UV–vis spectroscopy and computational analysis. The computed spectra and energies of the carbene and carbene complexes were in good agreement with the experimental data.

■ ASSOCIATED CONTENT

S Supporting Information. Figures S-1 to S-10; calculation of the equilibrium constant; complete reference to Gaussian 09; Table S-1; optimized geometries and energies for F₅-PhCCl, TMB, and F₅-PhCCl/TMB complexes A and B at the B97D/6-311+G(d) level. This material is available free of charge via the Internet at <http://pubs.acs.org>.

AUTHOR INFORMATION

Corresponding Author

*E-mail: moss@rutchem.rutgers.edu (R.A.M.); krogh@rutchem.rutgers.edu (K.K.-J.).

ACKNOWLEDGMENT

We are grateful to the National Science Foundation for financial support.

REFERENCES

- (1) (a) Tomioka, H.; Ozaki, Y.; Izawa, Y. *Tetrahedron* **1985**, *41*, 4987. (b) Ruck, R. T.; Jones, M., Jr. *Tetrahedron Lett.* **1998**, *39*, 2277. (c) Moss, R. A.; Yan, S.; Krogh-Jespersen, K. *J. Am. Chem. Soc.* **1988**, *120*, 1088. (d) Krogh-Jespersen, K.; Yan, S.; Moss, R. A. *J. Am. Chem. Soc.* **1999**, *121*, 6269.
- (2) Kahn, M. I.; Goodman, J. L. *J. Am. Chem. Soc.* **1995**, *117*, 6635.
- (3) (a) Tippmann, E. M.; Platz, M. S.; Svir, I. B.; Klymenko, O. V. *J. Am. Chem. Soc.* **2004**, *126*, 5750. (b) Wang, J.; Kubicki, J.; Peng, H.; Platz, M. S. *J. Am. Chem. Soc.* **2008**, *130*, 6604.
- (4) (a) Moss, R. A.; Tian, J.; Sauers, R. R.; Krogh-Jespersen, K. *J. Am. Chem. Soc.* **2007**, *129*, 10019. (b) Moss, R. A.; Wang, L.; Weintraub, E.; Krogh-Jespersen, K. *J. Phys. Chem. A* **2008**, *112*, 4651. (c) Moss, R. A.; Wang, L.; Odorisio, C. M.; Krogh-Jespersen, K. *J. Phys. Chem. A* **2010**, *114*, 209.
- (5) Moss, R. A.; Wang, L.; Odorisio, C. M.; Krogh-Jespersen, K. *J. Am. Chem. Soc.* **2010**, *132*, 10677.
- (6) Wang, L.; Moss, R. A.; Thompson, J.; Krogh-Jespersen, K. *Org. Lett.* **2011**, *13*, 1198.
- (7) Charton, M. *Prog. Phys. Org. Chem.* **1981**, *13*, 119; see also pp 143 and 149.
- (8) Charton, M. Private communication, Nov 22, 2010.
- (9) See ref 7, p 211.
- (10) Ehrenson, S.; Brownlee, R. T. C.; Taft, R. W. *Prog. Phys. Org. Chem.* **1973**, *10*, 1; see also p 13.
- (11) Admasu, A.; Gudmundsdottir, A. D.; Platz, M. S. *J. Phys. Chem. A* **1997**, *101*, 3832.
- (12) Matzinger, S.; Bally, T.; Patterson, E. V.; McMahon, R. J. *J. Am. Chem. Soc.* **1996**, *118*, 1535.
- (13) Pliego, J. R., Jr.; De Almeida, W. B.; Celebi, S.; Zhu, Z.; Platz, M. S. *J. Phys. Chem. A* **1999**, *103*, 7481.
- (14) (a) Garigipati, R. S. *Tetrahedron Lett.* **1990**, *31*, 1969. (b) Moss, R. A.; Ma, W.; Merrer, D. C.; Xue, S. *Tetrahedron Lett.* **1995**, *36*, 8761.
- (15) Graham, W. H. *J. Am. Chem. Soc.* **1965**, *87*, 4396.
- (16) Frisch, M. J., et al. *Gaussian 09, Revision A.02*; Gaussian, Inc.: Wallingford, CT, 2009. See the Supporting Information for the complete reference to *Gaussian 09*.
- (17) Parr, R. G.; Yang, W. *Density-Functional Theory of Atoms and Molecules*; University Press: Oxford, 1989.
- (18) Grimme, S. *J. Comput. Chem.* **2006**, *27*, 1787.
- (19) Zhao, Y.; Truhlar, D. G. *J. Phys. Chem. A* **2006**, *110*, 5121.
- (20) Chai, J.-D.; Head-Gordon, M. *Phys. Chem. Chem. Phys.* **2008**, *10*, 6615.
- (21) (a) Ditchfield, R.; Hehre, W. J.; Pople, J. A. *J. Chem. Phys.* **1971**, *54*, 721. (b) Hariharan, P. C.; Pople, J. A. *Mol. Phys.* **1974**, *27*, 209. (c) Krishnan, R.; Binkley, J. S.; Seeger, R.; Pople, J. A. *J. Chem. Phys.* **1980**, *72*, 650. (d) McLean, A. D.; Chandler, G. S. *J. Chem. Phys.* **1980**, *72*, 5639. (e) Clark, T.; Chandrasekhar, J.; Spitznagel, G. W.; Schleyer, P. v. R. *J. Comput. Chem.* **1983**, *4*, 294.
- (22) McQuarrie, D. A. *Statistical Thermodynamics*; Harper and Row: New York, 1973.
- (23) (a) Liu, B.; McLean, A. D. *J. Chem. Phys.* **1973**, *59*, 4557. (b) Boys, S. F.; Bernardi, F. *Mol. Phys.* **1970**, *19*, 553.
- (24) (a) Becke, A. D. *J. Chem. Phys.* **1993**, *98*, 5468. (b) Lee, C.; Yang, W.; Parr, R. G. *Phys. Rev. B* **1988**, *37*, 785.
- (25) Pople, J. A.; Head-Gordon, M.; Raghavachari, K. *J. Chem. Phys.* **1987**, *87*, 5968.
- (26) Mulliken, R. S. *J. Chem. Phys.* **1955**, *23*, 1833.
- (27) (a) Casida, M. E.; Jamorski, C.; Casida, K. C.; Salahub, D. R. *J. Chem. Phys.* **1998**, *108*, 4439. (b) See, e.g., Dreuw, A.; Weisman, J. L.; Head-Gordon, M. *J. Chem. Phys.* **2003**, *119*, 2943.
- (28) Barone, V.; Cossi, M. *J. Phys. Chem. A* **1998**, *102*, 1995.
- (29) Calibration corrects the raw UV-vis absorptions for wave-length-dependent variations in sample absorptivity, xenon monitoring lamp emission, and detector sensitivity.⁵ The calibration spectrum is shown in the Supporting Information (Figure S-2).
- (30) Results obtained at the TD-B3LYP/6-311+G(d)//B97D/6-311+G(d) level with SCRf = CPCM, solvent = pentane. See Section 2.2, above.
- (31) $K = (1/\text{slope}) (f_3/f_1)$, where f_3 (0.332) is the computed oscillator strength of F₅-PhCCl at 296 nm and f_1 (0.0829) is the computed oscillator strength of carbene complex B at 545 nm. See the Supporting Information for details.
- (32) Complexation of F₅-PhCCl by TMB ($K = 3.21 \times 10^5 \text{ M}^{-1}$) is slightly superior to complexation of *p*-O₂NPhCCl by TMB ($K = 1.34 \times 10^5 \text{ M}^{-1}$).⁶
- (33) Nguyen, T. L.; Kim, G. S.; Mebel, A. M.; Nguyen, M. T. *Chem. Phys. Lett.* **2001**, *349*, 571–577.
- (34) Woodcock, H. L.; Moran, D.; Brooks, B. R.; Schleyer, P. v. R.; Schaefer, H. F. *J. Am. Chem. Soc.* **2007**, *129*, 3763.
- (35) Koch, W.; Holthausen, M. C. *A Chemist's Guide to Density Functional Theory*; Wiley-VCH: Weinheim, 2000.
- (36) McKellar, A. R. W.; Bunker, P. R.; Sears, T. J.; Evenson, K. M.; Saykally, R. J.; Langhoff, S. R. *J. Chem. Phys.* **1983**, *79*, 5251.